DOI:10.1021/jf902509f

JOURNAL OF AGRICULTURAL AND FOOD CHEMISTRY
ARTICLE

Olive Fruit Growth and Ripening as Seen by Vibrational Spectroscopy

Macarena López-Sánchez, María José Ayora-Cañada,* and Antonio Molina-Díaz

Department of Physical and Analytical Chemistry, Faculty of Experimental Sciences, University of Jaén, 23071 Jaén, Spain

The aim of this work was to examine the potential of ATR-FTIR and Raman spectroscopies to evaluate changes happening during the development and maturation of olive fruit. To do this, the spectra of the different parts of the olive (skin, flesh and stone) have been measured at different stages of development. The evolution of different spectral bands has been related to the content of olive constituents like triglycerides, water, carotenoids and phenolic compounds. Oil accumulation can be followed using both FTIR and Raman spectroscopy. The increase in bands at 1746 cm^{-1} (ATR-FTIR) and 1440 cm^{-1} (Raman) correlates well with the oil content in the fruit determined using the standard Soxhlet extraction method. In the case of overripe olives ATR-FTIR does not provide a representative spectrum of the olive flesh due to the accumulation of water on the surface of the ATR crystal. The increase of the content in carotenoids and phenolic compounds during olive growing and their decrease during the ripening phase can be successfully monitored by means of the Raman bands at 1525 and 1605 cm^{-1}, respectively.

KEYWORDS: Olive growth; ripening; Raman spectroscopy; Fourier transform infrared spectroscopy; olive oil; carotenoids; polyphenols

1. INTRODUCTION

The olive tree (*Olea europaea* L.) is one of the most ancient domestic, cultivated plants characteristic of the Mediterranean basin and has an important economical impact for the production of olive oil. The quality of the oil is largely dependent on the composition of the olive fruits at harvesting because virgin olive oil is obtained by mechanical or physical methods (*1*, *2*). Olive fruit growth and maturation take place from the beginning of summer until the early winter. During this period, the olive undergoes different changes such as an increase in fruit weight and changes in color. The endocarp (pit or stone) enlarges to full size and hardens by six weeks after full bloom, whereas the mesocarp (flesh) and exocarp (skin) continue their gradual growth. Fruit begins changing from a green color to purple and finally black. Other processes happen inside the fruit, and are more difficult to evaluate, as the evolution of structural components like polysaccharides, mainly cellulose, hemicellulose and lignin, sugars, as well as other minor components as hydrocarbons, sterols, alcohols, chlorophylls, carotenoids and polar phenolic compounds, all present in the olive fruit.

The determination of several components at different maturity stages has been approached using different techniques like gas chromatography for triterpene alcohols and sterols (*3*) and HPLC for phenolics (*4*, *5*), chlorophyll and carotenoids (*6*) and organic acids (*7*). These and other studies involve the determination of individual components or groups of components, as in the case of spectrophotometric determination of total phenols (*4*). Magnetic resonance imaging of the olive fruit has been used to obtain information about the evolution of oil and water distribution at different stages of maturation (*8*, *9*). In this work, we propose the use of two vibrational spectroscopic techniques, FT-Raman and FTIR, to follow the evolution of different compounds during the olive fruit growth and maturation. Since spectral features in infrared and Raman spectra can often be assigned to specific chemical groups, these techniques provide molecular information. Thus, a more complete view, although much more general, of the process will be obtained. The great advantage of these techniques is, furthermore, the simplicity, or even total absence, of sample preparation, which makes them less demanding in terms of time and use of reagents than other methods, like chromatographic techniques.

Following the maturation progress with vibrational spectroscopic techniques, oil accumulation in the fruit could be easily monitored providing a rapid tool to classify olives depending on their maturation stage. This could be useful, for example, to diagnose if a fruit is mature enough to be collected, with a spectroscopic criteria, more objective than the visual inspection of the color changes.

2. MATERIALS AND METHODS

Instrumentation. Infrared spectra were acquired on a Tensor 27 (Bruker) Fourier transform infrared (FTIR) spectrometer which was equipped with a deuterated triglycine sulfate (DTGS) detector. Measurements were performed using a single-reflection diamond attenuated total reflection (ATR) accessory with sample pressure applicator

*To whom correspondence should be addressed. Phone: +34 953212937. Fax: +34 953212940. E-mail: mjayora@ujaen.es.

 Published on Web 11/16/2009

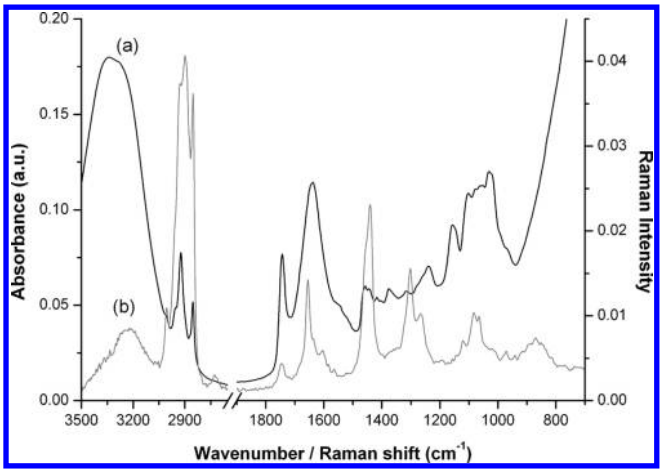

Figure 1. ATR-FTIR (**a**) and Raman (**b**) spectra of ripe olive flesh.

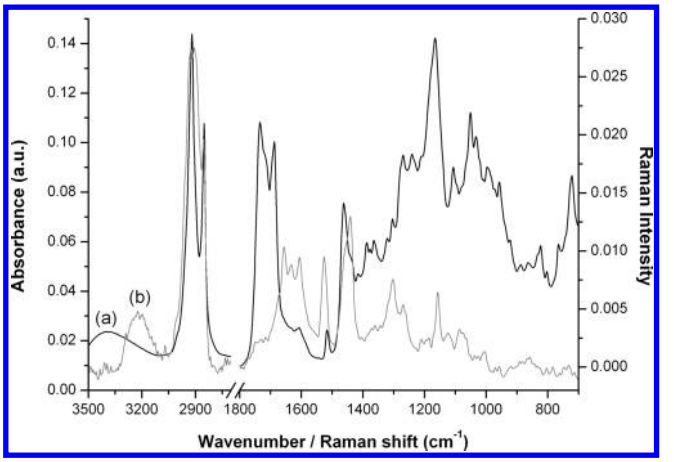

Figure 2. ATR-FTIR (**a**) and Raman (**b**) spectra of olive skin.

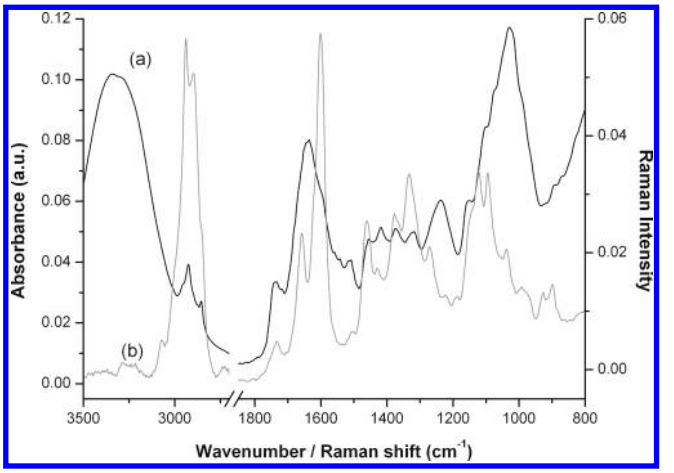

Figure 3. ATR-FTIR (**a**) and Raman (**b**) spectra of olive stone.

(DuraSamplIR). Scan number and resolution were optimized to 32 scans and 4 cm^{-1}, respectively, with a good signal-to-noise ratio. The spectrum of the clean and dry ATR element against air was used as background.

Raman spectra were recorded using a Bruker RFS FT-Raman spectrometer fitted with a liquid nitrogen cooled Ge detector. The excitation radiation was the 1064 nm line from a Nd:YAG laser (Coherent). All spectra were recorded with a resolution of 4 cm^{-1}, a laser power of 600 mW and 300 scans, using a focused laser beam. The Raman scattered radiation was collected at 180° geometry.

Sampling and Oil Extraction from Olives. Olives (picual variety) from the same olive tree were picked during the maturation process from June to February (around three samples of 100 g per month) during two consecutive crop seasons. Olives were washed with distilled water to remove dust from the surface and dried at room temperature.

Oil extraction from olive samples was performed using the Abencor method (*10*). This is a physical method that reproduces the industrial process of olive oil obtention in laboratory scale. It consists briefly in (a) milling the olives in a hammer mill, (b) malaxation of the produced olive paste by slow mixing during 30 min and (c) separation of the oil by centrifugation (*11*).

Spectroscopic Measurements. The different parts of the olive fruit, namely, the skin (epicarp), the flesh (mesocarp) and the stone (endocarp), were measured using attenuated total reflection Fourier transform infrared spectroscopy (ATR-FTIR) and Raman spectroscopy. Measurements of the skin were performed with intact fruits. Olives were sliced to record spectra of the flesh, and the stone was measured after removal of all the flesh around. Samples were just placed directly in the holder for Raman measurements. For ATR-FTIR measurements, it was necessary to make a controlled pressure, to ensure good contact between the sample and the diamond surface.

Raman and ATR-FTIR spectra of oil extracted from selected olive samples were recorded in a quartz cuvette and by placing a drop of the oil on top of the ATR crystal, respectively.

Reference Methods for Determination of Oil Content and Humidity. Oil content of the fruit was derived using the standard Soxhlet oil extraction method (*12*). This method is the most commonly used example of a semicontinuous method applied to the extraction of lipids from foods. According to the Soxhlet procedure, oil and fat from solid material were extracted by repeated washing (percolation) with an organic solvent (usually hexane or petroleum ether) under reflux for 4 h. The obtained oil was weighed to calculate the oil content (% of oil referred to dry matter).

To determine water contenty, 45 g of sample was dried for 12 h in an oven at 105 °C. The loss of weight gave the percentage of water and volatile matter of the sample (*13*).

3. RESULTS AND DISCUSSION

FTIR and Raman Spectra of the Different Parts of the Olive Fruit. Figure 1 shows the typical ATR-FTIR and Raman spectra of ripe olive flesh. In the FTIR spectrum, the most intense absorption bands (broad bands centered at *ca.* 3304 and 1636 cm^{-1}) correspond to water, which constitutes approximately 50% of the fruit weight. Water contributes less to the Raman spectrum. The C═O stretching band of ester bonds at 1746 cm^{-1} can be seen in both spectra, being much more intense in the FTIR spectrum.

Cellulosic, hemicelullosic and pectic polysaccharides of the cell walls give a complex fingerprint due to its characteristic bands in the 900−1200 cm^{-1} region of the infrared spectrum. These compounds contribute relatively little to the Raman spectra, which are dominated by bands attributable to lipids (*14*), in plane deformation $\delta(=C-H)$ of cis double bonds (1267 cm^{-1}), methylene twisting motion (1302 cm^{-1}), scissoring deformation of CH_2 (1441 cm^{-1}), C═C (cis RCH═CHR) stretching (1655 cm^{-1}). C−H stretching bands in the region 2900−3010 cm^{-1} are intense in both Raman and infrared spectra, whereas CH_2 deformation bands are weaker in the FTIR spectrum. The comparison between ATR-FTIR and FT-Raman spectra of the olive flesh shows up the complementary nature of both techniques.

Figure 2 shows ATR-FTIR and FT-Raman spectra of the olive skin. Epidermal cells are covered by the cuticle, a protective layer, which covers the olive fruit like most aerial parts of terrestrial plants. Both ATR-FTIR and FT-Raman spectra of olive skin are dominated by strong bands of long aliphatic chains (CH_2 bands at 2914, 2847, and 1472 cm^{-1}) typical of waxes (*15*). Additionally, the characteristic bands of polysaccharides are found in the region 900−1150 cm^{-1} of the infrared spectrum. Strong bands due to carbonyl groups can also be seen in the infrared spectrum in the region 1670−1740 cm^{-1}, whereas in Raman prominent bands due to C═C stretching appear between 1500 and 1670 cm^{-1}.

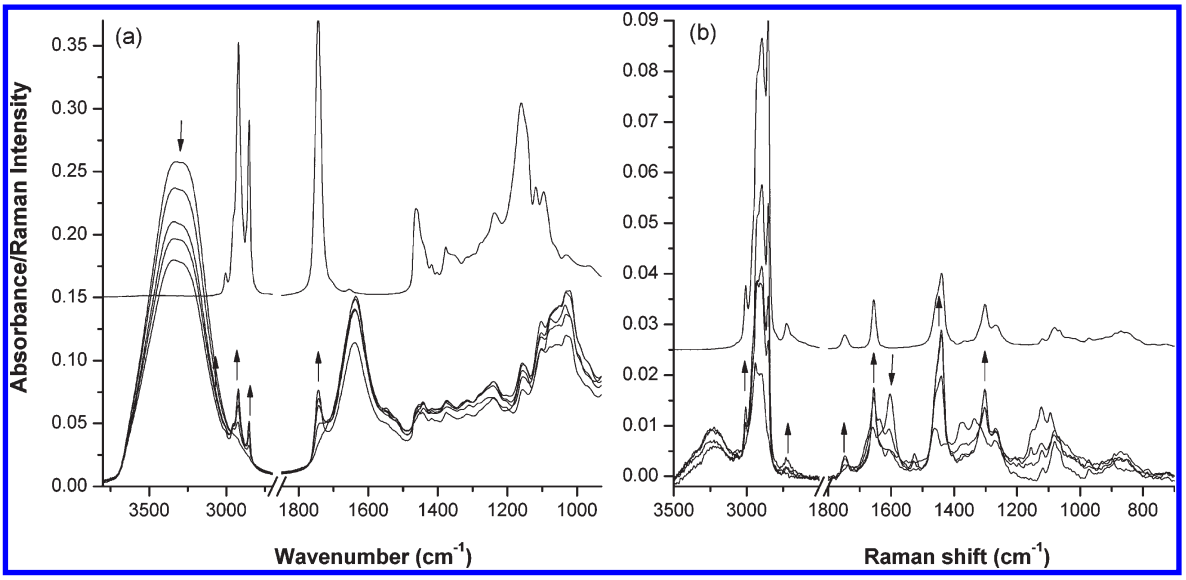

Figure 4. ATR-FTIR (**a**) and Raman spectra (**b**) of different olive flesh samples during development. ATR-FTIR and Raman spectra of olive oil are presented on top for comparison.

All these spectral features correspond to typical cuticle constituents. This layer is basically composed of pectopolysaccharides (pectin, cellulose and hemicellulose), cutin and waxes (*16*). The cutin matrix consists largely of esterified fatty acids, hydroxylated and epoxy-hydroxylated (*17*, *18*). Cuticular waxes are complex mixtures of homologous series of long-chain aliphatics such as alkanes, alcohols, aldehydes, fatty acids, and esters, with the addition of variable proportions of cyclic compounds such as triterpenoids and hydroxycinnamic acid derivatives (*17*, *19*).

Comparing the FTIR spectra of the skin and the flesh, one of the most remarkable differences is the absence of the characteristic water bands in the former. In fact, the cuticle is constituted mainly by hydrophobic compounds, representing a barrier between the intracellular and extracellular environment that prevents the diffusion of water and nutrients from the fruit (*20*).

Considering Raman spectra in the case of ripe olives, the flesh and skin spectral characteristics were more similar than for ATR-FTIR. This must be due to the fact that the laser penetration is higher in Raman and, when measuring the skin, bands belonging to the flesh are also observed. In ATR-FTIR, the measurement is done only in the outer part of the cuticle because the penetration depth of the evanescent wave is below few micrometers. Furthermore, the two characteristic Raman bands located at 1525 and 1157 cm^{-1} in the spectrum of the skin are due to carotenoid pigments, which occur in many fruits and vegetables and are very efficient Raman scatterers (*21*).

Finally, the olive stone or pit consists of a woody shell enclosing one or, rarely, two seeds. Its Raman spectra (**Figure 3b**) shows the characteristic bands of polymeric lignin (*21*, *22*), an amorphous polyphenolic material. The most intense band is due to the aromatic ring stretch at 1604 cm^{-1} with an accompanying band at 1658 cm^{-1}. The poor contact between the sample and the ATR crystal made difficult the acquisition of good quality infrared spectra due to the hardness of the olive stone. The obtained spectra (see **Figure 3a**) are dominated by typical bands of holocellulosic materials in the 900−1200 cm^{-1} region (*23*). The band of aromatic ring stretch of lignin should appear in the same location as in the Raman spectrum. However, this region was obscured by the strong water deformation band centered at 1638 cm^{-1}. The typical infrared pattern of lignocellulosic materials is observed in the region 900−1200 cm^{-1}.

Complete information about the different parts of the olive fruit has been derived from Raman and infrared spectra. Thus, the combined use of both techniques is of interest in order to obtain the maximum information on changes during the growth and ripening processes.

Spectral Changes during Olive Growing and Ripening. Several changes were observed in the vibrational spectra of the olive flesh, skin and stone during the growth and ripening process from June to February. The most significant changes happened in the flesh, where oil accumulation takes place. Selected ATR-FTIR and Raman spectra of the flesh, together with olive oil spectra, are shown in **Figure 4**.

The accumulation of oil during the growing process can be easily followed by monitoring the characteristic spectral bands of lipids. For comparison, the area of characteristic infrared and Raman bands of oil and water has been plotted versus time together with results of oil and water content from reference analysis (**Figure 5**). Three different stages can be distinguished: (a) Before stone hardening or lignification (day 0) no changes are observed in oil bands; this phase corresponds to a period of rapid fruit growth involving mainly growth and development of the endocarp (seed/stone), with little flesh development until endocarp cells stop dividing and become sclerified (*24*). (b) Then, a rapid increase of characteristic oil bands in both ATR-FTIR and Raman spectra occurs from July to October. The tendency is similar to that revealed by Sohlext measurements and corresponds to an intense oil biosynthesis period with mesocarp development mainly by expansion of pre-existing flesh cells due to oil accumulation. (c) Finally, stabilization of oil content is clearly observed in reference analysis and Raman results. As the fruit ripens, oil synthesis continues but at a much slower rate. However, in ATR-FTIR, the area of the oil band does not remain constant after 100 days but a sudden decrease is observed in **Figure 5**. This decrease is accompanied by an increase in the characteristic water band. This observation does not correspond with the results of Raman spectroscopy and the reference analysis. This anomalous behavior of infrared measurements must be attributed to the particular characteristics of the ATR technique. For ATR measurements, the contact of the sample with the surface of the ATR crystal is decisive. It seems that cells broke due to the applied

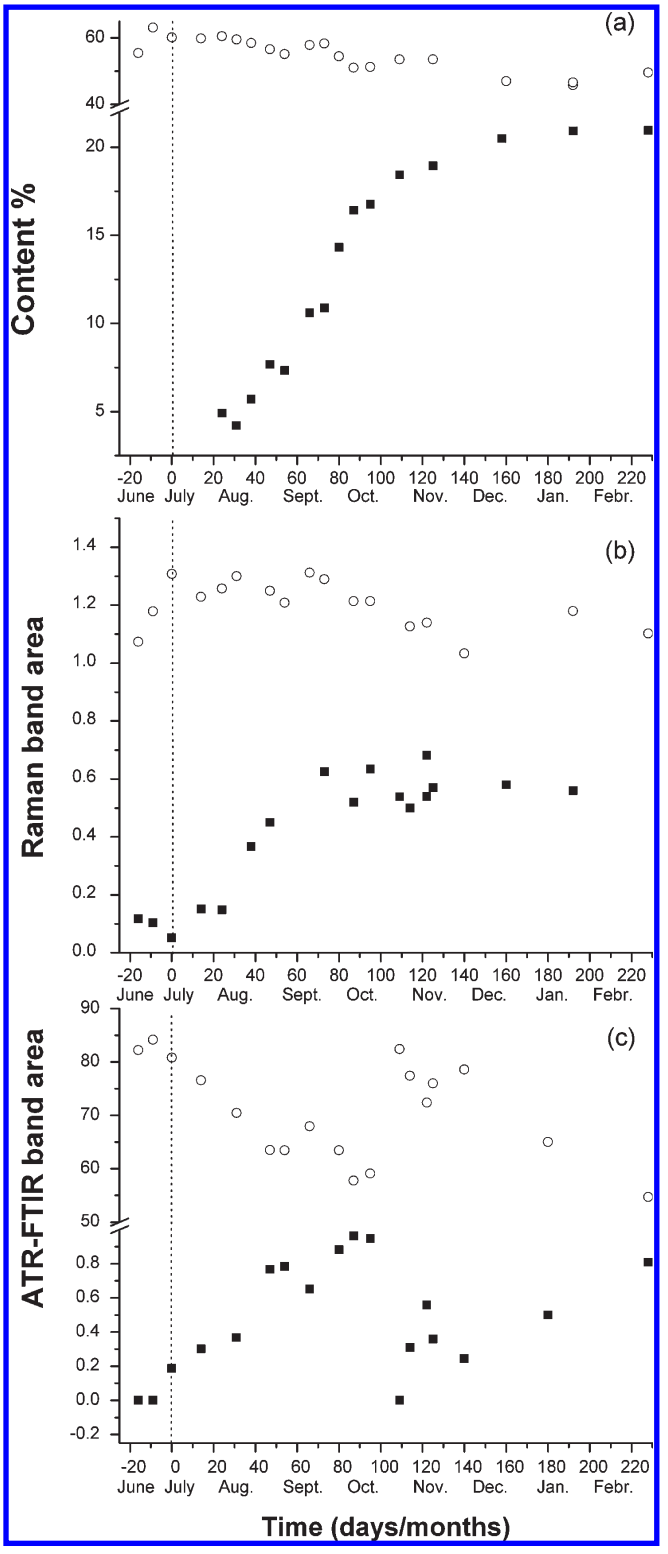

Figure 5. Oil (■) and water (○) content evolution during fruit development and ripening. (**a**) Data from reference methods. (**b**) Raman characteristic bands: 1440 cm^{-1} (oil) 3250 cm^{-1} (water). (**c**) ATR-FTIR characteristic bands: 1746 cm^{-1} (oil) and 3300 cm^{-1} (water).

pressure when measuring and water could partially displace oil at the ATR crystal surface due to its higher density. This only happened when olives were ripe enough because during ripening a rapid change in fruit texture takes place and the fruit loses firmness as a consequence of the modification of the cell wall components that is caused by endogenous enzymes (*25*).

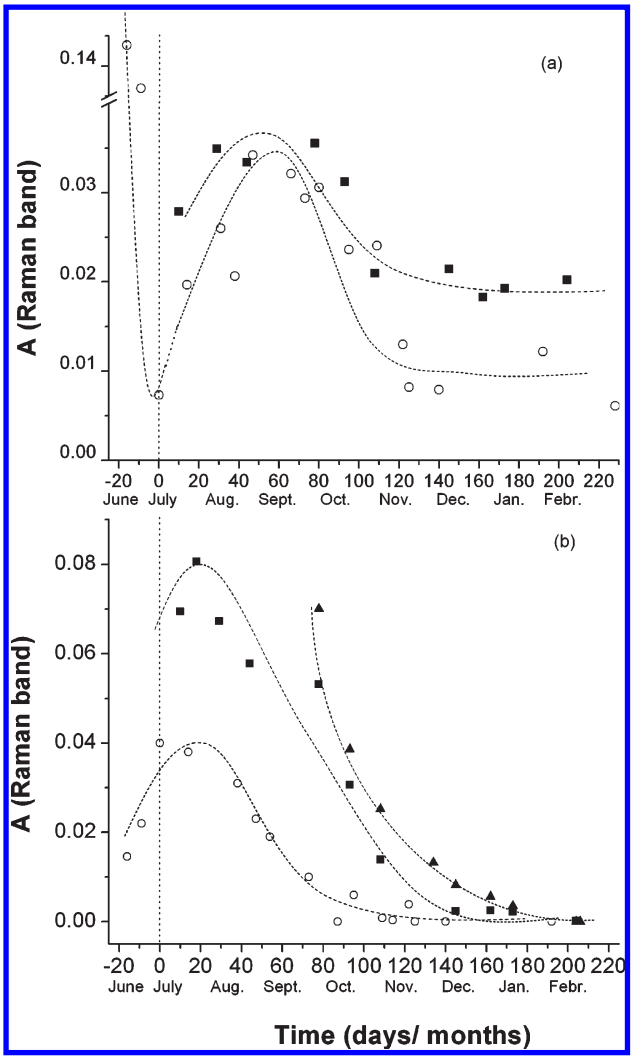

Figure 6. Evolution of Raman band areas of (**a**) aromatics (1605 cm^{-1}) and (**b**) carotenoids (1525 cm^{-1}) in oil and olives during development and ripening [(○) olives, first harvest; (■) olives, second harvest; (▲) oil, first harvest].

From these observations it can be concluded that Raman spectroscopy is more appropriate for the measurement of ripe olives than ATR-FTIR. Apart from oil accumulation, changes in other compounds during olive growing and ripening can also be monitored using Raman spectroscopy (see **Figure 6**).

Phenolic compounds give a characteristic Raman band at 1605 cm^{-1} due to conjugated C−C vibrations of aromatic rings. This band follows a characteristic pattern during olive growth and ripening as can be seen in **Figure 6a** for two different harvests. Similar trends are observed for both harvests although slight differences occur due to climatologic conditions. Data corresponding to olives before stone lignification are available only for one of the harvests. An abrupt decrease in aromatic content is observed during this period. After stone lignification (day 0), the same tendency is observed for both harvest years. There was a moderate increase followed by a decrease and a final stabilization. To interpret these tendencies a double origin of the band characteristic of aromatics must be considered. Before stone lignification, the high content of aromatics in the flesh can be attributed to lignin precursors. Lignification of plant cell walls involves monolignol formation, transportation and polymerization to form complex three-dimensional phenolic polymers that are generally termed as lignin. Thus, the characteristic doublet at

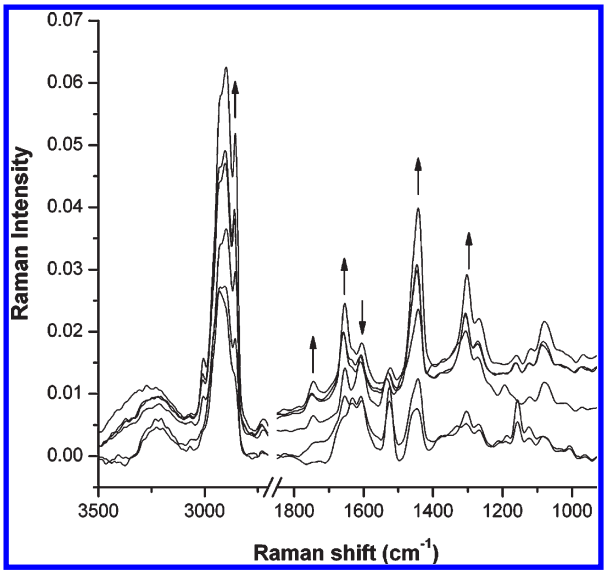

Figure 7. Evolution of Raman spectra of intact olives during fruit development.

1603 and 1630 cm^{-1} of ferulic acid (*26*), an intermediate in the synthesis of monolignols, is clearly observed in the Raman spectra of the olives before lignification. After stone lignification the behavior of the Raman band of aromatics coincides with changes in the phenolic content. Several studies have reported that the concentration of total phenols progressively increases to a maximum level and then decreases sharply as ripening progresses and the fruit blackens (*24*, *27*, *28*). The last phase coincides with the period of oil content stabilization. The observation of changes in this region of the infrared spectrum was hindered by the strong absorption of water.

Carotenoid evolution can also be followed by plotting the band centered at 1525 cm^{-1}, which corresponds to the C=C stretching in highly conjugated double bond systems (see **Figure 6b**). This band together with another one at 1155 cm^{-1}, assigned to C−C stretching, is typical of carotenoids (*21*, *29*). As it happened with aromatics, the same tendency is observed for both harvests. In this case, the amount is higher in one of them probably due to the differences in climatologic conditions during crop years. The carotenoid content increases progressively during the first weeks of fruit growth, until the fruit is fully developed. Then the content begins to fall relatively rapidly, coinciding with the loss of the green color of the olives and the development of the black color due to the progressive synthesis of anthocyanin compounds. In olives, although the content of carotenoids is low, their presence is important because, together with the chlorophylls, they supply the characteristic color to virgin olive oil. The typical Raman band of carotenoids is also visible in the spectra of the extracted oil. The intensity is slightly higher than in olives due to the preconcentration of these compounds in the oil because of their liposoluble character. The temporal evolution is similar to that seen for the olive fruit as a whole.

Considering the spectra of the skin of intact olives, the Raman bands of carotenoids (1525 and 1157 cm^{-1}) also decreased markedly during ripening. It is also remarkable that, as the time passed, the skin was getting thinner and the spectra of intact mature olives contained more contribution from flesh constituents. This is an interesting observation because it demonstrates that the measurement of intact olives using Raman spectroscopy can be useful for the monitoring of oil accumulation inside the flesh, as can be seen in **Figure 7**.

In conclusion, vibrational spectroscopic techniques, and especially Raman spectroscopy, are useful to monitor olive fruit growing and ripening. By means of them, changes in the content of different components, such as lipids, water, carotenoids or phenolic compounds, can be monitored in a simple and rapid way. Thus, the kinetics of oil accumulation during the growing phase can be much more easily followed using the proposed spectroscopic techniques than employing the traditional methods that have been used as reference. In addition, the evolution of the content of phenolic compounds and carotenoids derived from the Raman spectra can be an important indicator of the optimum harvest time.

LITERATURE CITED

(1) Beltran, G.; Aguilera, M. P.; Rio, C. D.; Sanchez, S.; Martinez, L. Influence of fruit ripening process on the natural antioxidant content of Hojiblanca virgin olive oils. *Food Chem.* **2005**, *89*, 207–215.

(2) Yousfi, K.; Cert, R. M.; Garcia, J. M. Changes in quality and phenolic compounds of virgin olive oils during objectively described fruit maturation. *Eur. Food Res. Technol.* **2006**, *223*, 117–124.

(3) Sakouhi, F.; Absalon, C.; Sebei, K.; Fouquet, E.; Boukhchina, S.; Kallel, H. Gas chromatographic-mass spectrometric characterisation of triterpene alcohols and monomethylsterols in developing Olea europaea L. fruits. *Food Chem.* **2009**, *116*, 345–350.

(4) Bonoli, M.; Bendini, A.; Cerretani, L.; Lercker, G.; Toschi, T. G. Qualitative and semiquantitative analysis of phenolic compounds in extra virgin olive oils as a function of the ripening degree of olive fruits by different analytical techniques. *J. Agric. Food Chem.* **2004**, *52*, 7026–7032.

(5) Morello, J. R.; Romero, M. P.; Motilva, M. J. Effect of the maturation of the olive fruit on the phenolic fraction of drupes and oils from Arbequina, Farga, and Morrut cultivars. *J. Agric. Food Chem.* **2004**, *52*, 6002–6009.

(6) Criado, M. N.; Motilva, M. J.; Goni, M.; Romero, M. P. Comparative study of the effect of the maturation process of the olive fruit on the chlorophyll and carotenoid fractions of drupes and virgin oils from Arbequina and Farga cultivars. *Food Chem.* **2007**, *100*, 748–755.

(7) Nergiz, C.; Ergönül, P. G. Organic acid content and composition of the olive fruits during ripening and its relationship with oil and sugar. *Sci. Hortic.* **2009**, *122*, 216–220.

(8) Brescia, M. A.; Pugliese, T.; Hardy, E.; Sacco, A. Compositional and structural investigations of ripening of table olives, Bella della Daunia, by means of traditional and magnetic resonance imaging analyses. *Food Chem.* **2007**, *105*, 400–404.

(9) Gussoni, M.; Greco, F.; Consonni, R.; Molinari, H.; Zannoni, G.; Bianchi, G.; Zetta, L. Application of NMR microscopy to the histochemistry study of olives (Olea europaea L.). *Magn. Reson. Imaging* **1993**, *11*, 259–268.

(10) Martínez, J. M.; Muñoz, E.; Alba, J.; Lanzón, A. Informe sobre utilización del analizador de muestras Abencor. *Grasas Aceites* **1975**, *26*, 379–385.

(11) Guardia-Rubio, M.; Marchal-López, R.; Ayora-Cañada, M. J.; Ruiz-Medina, A. Determination of pesticides in olives by gas chromatography using different detection systems. *J. Chromatogr. A* **2007**, *1145*, 195–203.

(12) UNE 55032 Normas UNE, Asociación Española de Normalización y Certificación (AENOR), **1973**.

(13) IOOC, IUPAC; Method 2601 or ISO 662, **1980**.

(14) Muik, B.; Lendl, B.; Molina-Diaz, A.; Ayora-Cañada, M. J. Fourier transform Raman spectrometry for the quantitative analysis of oil content and humidity in olives. *Appl. Spectrosc.* **2003**, *57*, 233–237.

(15) Ribeiro da Luz, B. Attenuated total reflectance spectroscopy of plant leaves: A tool for ecological and botanical studies. *New Phytol.* **2006**, *172*, 305–318.

(16) Dominguez, E.; Heredia, A. Water hydration in cutinized cell walls: A physico-chemical analysis. *Biochim. Biophys. Acta* **1999**, *1426*, 168–176.

(17) Heredia, A. Biophysical and biochemical characteristics of cutin, a plant barrier biopolymer. *Biochim. Biophys. Acta* **2003**, *1620*, 1–7.
(18) Kolattukudy, P. E. Polyesters in higher plants. *Adv. Biochem. Eng. Biotechnol.* **2001**, *71*, 1–49.
(19) Bianchi, G.; Vlahov, G.; Anglani, C.; Murelli, C. Epicuticular wax of olive leaves. *Phytochemistry* **1992**, *32*, 49–52.
(20) Martin,J. T.Juniper,B. E. *The cuticles of plants*; St. Martin's Press: New York, 1970.
(21) Schrader, B.; Klump, H. H.; Schenzel, K.; Schulz, H. Non-destructive NIR FT raman analysis of plants. *J. Mol. Struct.* **1999**, *509*, 201–212.
(22) Morrison, W. H.III; Himmelsbach, D. S.; Akin, D. E.; Evans, J. D. Chemical and spectroscopic analysis of lignin in isolated flax fibers. *J. Agric. Food Chem.* **2003**, *51*, 2565–2568.
(23) Pandey, K. K. A Study of Chemical Structure of Soft and Hardwood and Wood Polymers by FTIR Spectroscopy. *J. Appl. Polym. Sci.* **1999**, *71*, 1969–1975.
(24) Conde, C.; Delrot, S.; Gerós, H. Physiological, biochemical and molecular changes occurring during olive development and ripening. *J. Plant Physiol.* **2008**, *165*, 1545–1562.
(25) Heredia, A.; Fernandez-Bolanos, J.; Guillen, R. Cellulase inhibition by polyphenols in olive fruits. *Food Chem.* **1990**, *38*, 69–73.
(26) Piot, O.; Autran, J. C.; Manfait, M. Spatial Distribution of Protein and Phenolic Constituents in Wheat Grain as Probed by Confocal Raman Microspectroscopy. *J. Cereal Sci.* **2000**, *32*, 57–71.
(27) Rotondi, A.; Bendini, A.; Cerretani, L.; Mari, M.; Lercker, G.; Toschi, T. G. Effect of olive ripening degree on the oxidative stability and organoleptic properties of cv. Nostrana di Brisighella extra virgin olive oil. *J. Agric. Food Chem.* **2004**, *52*, 3649–3654.
(28) Jemai, H.; Bouaziz, M.; Sayadi, S. Phenolic composition, sugar contents and antioxidant activity of Tunisian sweet olive cultivar with regard to fruit ripening. *J. Agric. Food Chem.* **2009**, *57*, 2961–2968.
(29) Vershinin, A. Carotenoids in mollusca:approaching the functions. *Comp, Biochem, Physiol,* **1996**, *113B*, 63–71.

Received for review July 21, 2009. Revised manuscript received September 25, 2009. Accepted October 26, 2009. M.L.-S. is grateful for a predoctoral fellowship from Junta de Andalucía (Spain).